JACS
JOURNAL OF THE AMERICAN CHEMICAL SOCIETY
Article
pubs.acs.org/JACS

Microfluidic Screening of Electrophoretic Mobility Shifts Elucidates Riboswitch Binding Function

Kelly Karns,[†] Jacob M. Vogan,[‡] Qian Qin,[§] Scott F. Hickey,[§] Stephen C. Wilson,[§] Ming C. Hammond,*[,‡,§] and Amy E. Herr*[,†,∥]

[†]San Francisco Graduate Program in Bioengineering, University of California, Berkeley−University of California, [‡]Department of Molecular & Cell Biology, [§]Department of Chemistry, and [∥]Department of Bioengineering, University of California, Berkeley, California 94720, United States

Supporting Information

ABSTRACT: Riboswitches are RNA sensors that change conformation upon binding small molecule metabolites, in turn modulating gene expression. Our understanding of riboswitch regulatory function would be accelerated by a high-throughput, quantitative screening tool capable of measuring riboswitch−ligand binding. We introduce a microfluidic mobility shift assay that enables precise and rapid quantitation of ligand binding and subsequent riboswitch conformational change. In 0.3% of the time required for benchtop assays (3.2 versus 1020 min), we screen and validate five candidate SAM-I riboswitches isolated from thermophilic and cryophilic bacteria. The format offers enhanced resolution of conformational change compared to slab gel formats, quantitation, and repeatability for statistical assessment of small mobility shifts, low reagent consumption, and riboswitch characterization without modification of the aptamer structure. Appreciable analytical sensitivity coupled with high-resolution separation performance allows quantitation of equilibrium dissociation constants (K_d) for both rapidly and slowly interconverting riboswitch−ligand pairs as validated through experiments and modeling. Conformational change, triplicate mobility shift measurements, and K_d are reported for both a known and a candidate SAM-I riboswitch with comparison to in-line probing assay results. The microfluidic mobility shift assay establishes a scalable format for the study of riboswitch−ligand binding that will advance the discovery and selection of novel riboswitches and the development of antibiotics to target bacterial riboswitches.

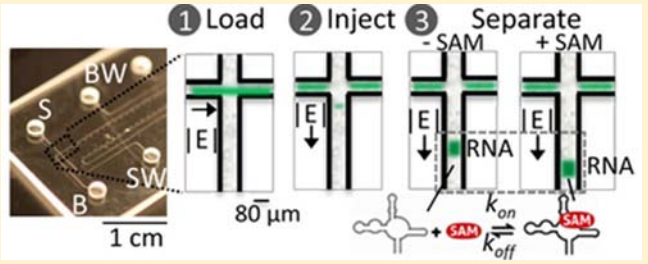

INTRODUCTION

Molecular conformation is fundamental to gene expression. In particular, localized RNA conformational changes upon ligand binding are critical to riboswitch-mediated gene control. Riboswitches are *cis*-acting RNA elements composed of both an aptamer and expression platform domain. These RNA molecules undergo a conformational change when bound to small molecule metabolites or ligands.[1,2] Conformation changes confer gene regulation mainly by terminating transcription (e.g., through formation of a terminator hairpin) or inhibiting translation initiation (e.g., through sequestration of the Shine−Dalgarno sequence).[2] First discovered just a decade ago,[3] only a handful of riboswitches have been identified, warranting further discovery and characterization efforts. Understanding these conserved gene regulatory mechanisms may profoundly impact diverse efforts including developing next-generation antibiotics,[4] designing genetic circuitry for synthetic biology applications,[5] and generating RNA-based biosensors.[6]

Given the importance of these molecules and the computational power of current bioinformatics tools, the number of *in silico* predicted riboswitches has surged.[7,8] Subsequent experimental validation of putative riboswitches relies on benchtop assays that determine ligand binding through various means, including observation of RNA conformational change via in-line probing,[9] 2-aminopurine fluorescence,[10,11] and Förster resonance energy transfer (FRET),[12] change in heat of the reaction via isothermal calorimetry,[13] or ligand diffusion via equilibrium dialysis.[14] While suitable for low-throughput biophysical measurements, these conventional riboswitch analytical tools have notable limitations, such as requiring lengthy incubation times, large sample sizes, or site-specific labeling of the ligand or the RNA, all of which slow down analytical throughput.

A binding assay that obviates the need for site-specific labeling of the ligand or the RNA is native polyacrylamide gel electrophoresis (PAGE). Native PAGE is extensively employed to study protein−protein,[15] protein−nucleotide,[16] and nucleotide−small molecule[10] interactions. Slab gel native PAGE has been used to confirm protein-free riboswitch-metabolite binding and altered RNA conformation through an observed change in riboswitch aptamer electrophoretic mobility ('mobility shift').[17,18] The mobility shift typically stems from the more compact structure of the ligand-bound riboswitch aptamer as compared to unbound RNA. Thus, the compact, bound

Received: October 31, 2012
Published: January 23, 2013

riboswitch exhibits a faster apparent electrophoretic mobility than the unbound RNA (Figure 1A).

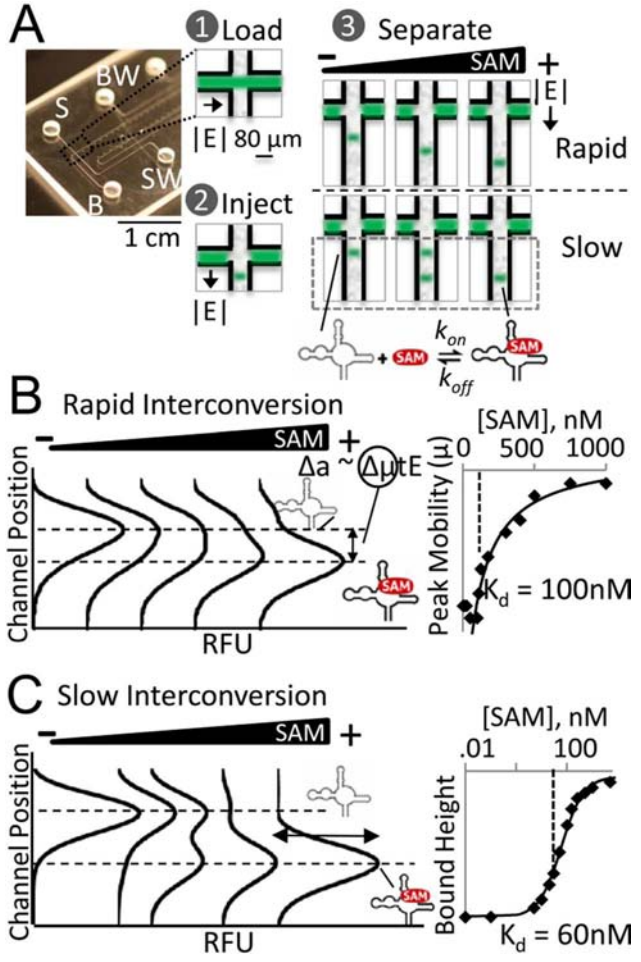

Figure 1. Microfluidic mobility shift assay (μMSA) screening capability spans multiple transport and interconversion regimes. (A) Sample is electrophoretically loaded, injected, and separated on-chip. SAM ligand binding to SAM-I riboswitches induces a conformational change in the RNA molecule and faster electrophoretic mobility. The observed band pattern, as ligand concentration is increased, is dependent on the interconversion rate relative to the separation time scale. Simulation results show different separation regimes for rapid (B) versus slow (C) interconversion between bound and free states. When riboswitch interconversion is rapid compared to assay time scales, simulation results show a single mobility-shifted RNA peak. Where riboswitch interconversion is negligible, simulation results show two resolved RNA peaks. K_d can be determined in both cases by tracking peak mobility (B) or bound peak height (C). In (B), k_{on} is 4.55 s^{-1} μM^{-1} and k_{off} is 0.455 s^{-1} or $\log(Da_{on}) = 2$ and $\log(Da_{off}) = 1$. In (C), k_{on} is 2.22 s^{-1} μM^{-1} and k_{off} is 2×10^{-6} s^{-1} or $\log(Da_{on}) = 2$ and $\log(Da_{off}) = -4$.

However, the workhorse native PAGE slab gel assay is unsuitable for high-throughput screens needed to experimentally validate candidate riboswitches and explore promising regions of the prediction space. Further, native PAGE slab gels often lack the resolving power required to separate molecular populations with small mobility shifts or those that differ in conformation rather than weight. Perhaps most important to riboswitch functional validation, slab gel native PAGE lacks the quantitation capacity essential to generate a robust, detailed understanding of riboswitch function and binding affinity. In contrast, microfluidic electrophoretic assays offer run-to-run repeatability and a degree of precision not attainable with slab gel formats. While microfluidic integration and automation has begun to benefit drug screening,[19] developmental biology,[20,21] and cell sorting for cancer research,[22] neither the throughput nor precision of on-chip PAGE have been harnessed for quantitative characterization of riboswitch–ligand binding interactions.

Consequently, we introduce an efficient riboswitch microfluidic mobility shift assay (μMSA) which advances beyond slab gel mobility shift assays by reporting ligand binding and riboswitch conformational change quickly (3 min) and quantitatively (Figure 1). Coupled with high-sensitivity fluorescence-based detection, we show that the microfluidic assay allows enhanced resolution of conformational change and enables riboswitch discovery and characterization without modification of the riboswitch aptamer structure. The enhanced analytical performance is also shown to enable quantification of equilibrium binding constants (K_d) spanning slowly to rapidly interconverting riboswitch–ligand pair targets. Lastly, we apply the riboswitch screening platform to functional analysis of five computationally predicted but previously unvalidated SAM-I riboswitches; completing the screening process with unmatched precision, reproducibility, and sparing resource consumption.

RESULTS AND DISCUSSION

Microfluidic Mobility Shift Assay Design: Screening Rapidly and Slowly Interconverting Binding Pairs. To introduce a broadly relevant riboswitch screening tool, we sought to design a native PAGE mobility shift assay capable of: (i) high-precision peak shift measurements appropriate for assessment of the small anticipated mobility shifts associated with RNA conformation change; (ii) repeatable operation to allow tests of statistical significance for observed mobility shifts; (iii) resource-sparing operation (material, time, handling) to afford assay scalability for screening uses; and (iv) quantifying K_d for a broad range of riboswitch–ligand binding kinetics. Here we detail salient design considerations for μMSA noting that while we focus attention on K_d determination for the ligand *S*-adenosylmethionine (SAM) binding to a set of fluorescently labeled known or putative SAM-I riboswitch aptamers, the assay platform is conversely well-suited to screening of a single putative riboswitch against a library of ligands.

We first sought to introduce a riboswitch functional screening assay optimized for measurement of K_d. For K_d determination, the RNA concentration typically must be significantly less than the expected K_d value,[23] making analytical sensitivity an important design specification for this screening assay. To meet this specification, we combine sensitive laser-induced fluorescence (LIF) detection with fast microfluidic PAGE separations. High-electric field PAGE, realizable due to excellent heat dissipation on the micro scale, yields fast separations which reduce the time for band broadening arising from molecular diffusion. To quantify the overlap of two peaks of interest, we use separation resolution ($R_s = \Delta a/(2\sigma_1 + 2\sigma_2)$, where Δa is the distance between the peaks and σ_1 and σ_2 are the bound and unbound peak widths, respectively). When $R_s > 0.5$, the peaks are considered resolved.[24] Combined with LIF, the rapid assay yields high signal-to-noise ratios (>3) even for picomolar RNA concentrations. Under these conditions, a single assay run completes in 12 s compared to 17 h on a slab

dx.doi.org/10.1021/ja310742m | J. Am. Chem. Soc. 2013, 135, 3136–3143

gel format, translating to detection of 40× smaller mobility shifts as compared to slab gels (Figure S1).

Next we sought to design electrophoretic separations capable of probing riboswitch−ligand binding interactions spanning rapidly to slowly interconverting systems (i.e., interconversion between bound and unbound forms). The speed of interconversion is important, as the Damkohler (Da) number indicates whether one or two peaks are expected. Thus, in turn, the Da number informs method selection for K_d determination using electrophoresis. Following convention, we define two Da numbers for electrophoretic separations of bound and unbound riboswitch populations as: $Da_{on} = k_{on}Lc_L/E\mu_A$ and $Da_{off} = k_{off}L/E\mu_A$, where k_{on} and k_{off} are the association and dissociation rate constants, respectively, L is the length scale of separation, E is the electric field, c_L is the concentration of ligand, and μ_A is the mobility of unbound riboswitch. The Peclet number (Pe = $L\mu E/D$) is ∼500 for all μMSA simulations and data and ∼800 for all slab gel data. Since K_d is a ratio of the rates of dissociation and association, binding pairs with similar K_d values can be either fast or slow interconverting species (Figures 1B,C and S2). We consider both cases.

In the case of slow interconversion (e.g., $Da_{on} > 1$ and $Da_{off} < 1$), two peaks corresponding to distinct bound and unbound RNA populations are resolvable ($R_s > 0.5$) by native PAGE (Figures 1C and S3). When the fluorescently labeled RNA is in excess, two populations are resolvable, since riboswitch−ligand association is rapid, while dissociation is slow in this regime; meaning that bound species stay bound throughout the characteristic electrophoresis time.[25,26] Thus, in the slow interconversion regime K_d is determined by measuring the peak height for the bound population of conformers as ligand concentration is increased. This method has been previously utilized to measure antibody−antigen K_d on-chip via native PAGE.[27]

In the rapid interconversion regime (Da_{on}, $Da_{off} > 1$), bound and unbound populations are predicted to overlap ($R_s < 0.5$), yielding a single riboswitch peak via native PAGE analysis (Figures 1B and S3). The riboswitch population forms a single peak as the association and dissociation times for the riboswitch−ligand interaction are fast compared to the time scale of electrophoresis. Thus, the mobility of this single peak corresponds to the population-average of bound riboswitches.[25,26] In this regime, K_d is determined by tracking the electrophoretic mobility of the single riboswitch band as ligand concentration is increased. In both regimes, free ligand will move with a fast electrophoretic mobility, owing to its small size, but the observed interconversion regimes will occur independent of ligand mobility. In this system, free ligand, free RNA, and bound RNA were not assumed to have the same electrophoretic mobility.

With these transport and reaction considerations in mind, we describe development of μMSA for K_d determination of a rapidly interconverting riboswitch−ligand binding pair (a validated SAM-I riboswitch from *Bacillus subtilis*), then of a slowly interconverting pair (a putative SAM-I riboswitch from *Polaribacter irgensii*). We then apply the new tool to functional screening of putative, computationally predicted SAM-I riboswitches.

Quantitative Analysis of Rapidly Interconverting Riboswitch States: A Validated SAM-I Riboswitch from *B. subtilis*. We first studied the mobility shift of and assessed the K_d for a previously confirmed 124 yitJ SAM-I riboswitch aptamer isolated from *B. subtilis* (*Bs*, Figure 2) that rapidly

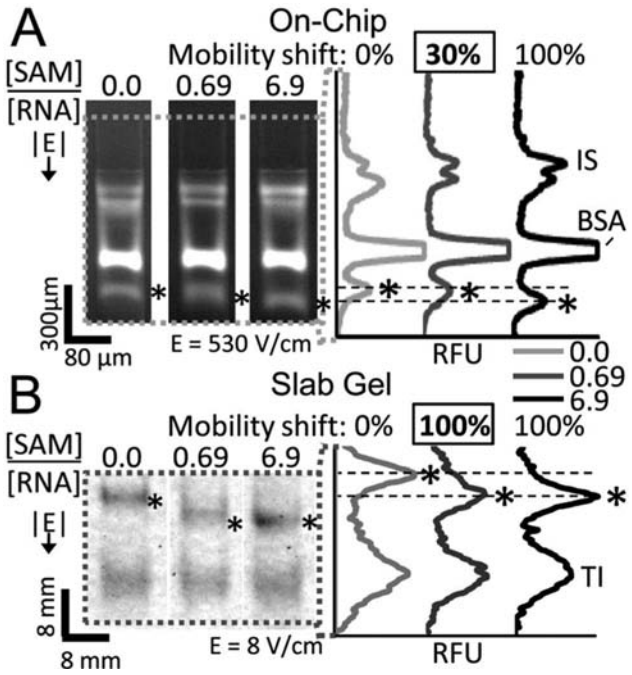

Figure 2. Microfluidic assay resolves a single mobility-shifted riboswitch peak in response to increasing ligand concentration (A) that is not resolvable on a slab gel (B). At a ligand:RNA ratio of 0.69, μMSA detects the SAM-I *Bs* riboswitch band at 30% of maximum mobility, while on the slab gel, the band appears fully shifted. BSA, TI, and IS are internal standard peaks, and '*' corresponds to the SAM-I *Bs* riboswitch band. Dashed lines correspond to minimally (0%) and maximally (100%) shifted RNA peak locations. 1× TB + 10 mM Mg^{2+} in gel and run buffers. RNA is labeled with AF488 (A) and FITC (B).

interconverts between bound and free states.[28] The mobility shift of the single peak was measured for increasing concentrations of SAM ligand with both μMSA and slab gel mobility shift formats. At a ligand:riboswitch ratio of 0.69, μMSA detected a single peak with a mobility 30% of the maximum mobility when binding is saturated (Figure 2A). At the same ligand:riboswitch ratio, the slab gel reported a single SAM-I *Bs* riboswitch band with maximally shifted mobility (Figure 2B). Consistent with our model for rapidly interconverting binding pairs, a single band was observed in both formats. In this regime the band mobility represents the fraction of bound RNA to total RNA.[26] The bound RNA population increases as ligand concentration increases, thus increasing the measured peak mobility until all the RNA molecules are bound and the peak is fully shifted. Unlike the slab gel, μMSA's ability to resolve intermediate peak mobilities suggests the microfluidic assay is capable of determining the riboswitch−ligand equilibrium dissociation constant (K_d). This lack of resolving power on a slab gel format also was observed for native PAGE analysis of the SAM-II riboswitch at intermediate ligand concentrations.[17]

In addition to needing to resolve intermediate mobility shifts as ligand concentration is increased, the binding assays are performed at RNA concentrations less than the K_d value and lower than the ligand concentrations in order to simplify the assessment of K_d. The μMSA lower limit of detection (LLOD) was 870 pM of RNA in 1 μL of sample detected using laser-induced fluorescence (signal-to-noise ratio = 5.3, labeling efficiency of 0.45 AlexaFluor-633 dye molecules per RNA molecule, detection at 1 mm separation distance, 3−12% PA

dx.doi.org/10.1021/ja310742m | J. Am. Chem. Soc. 2013, 135, 3136−3143

gel). This translates to 391.5 amol of fluorescently labeled RNA. Using a laser-induced fluorescence scanner, we determined the LLOD for the slab gel format to be approximately 0.75 pmol for fluorescently labeled RNA (labeling efficiency of 0.75 fluorophore dye molecules per RNA molecule). Typical slab gel LLOD is 4.8 fmol of radiolabeled RNA.[29] The μMSA platform thus yields a 1916-fold sensitivity improvement over a slab gel format for fluorescently labeled RNA and comparable sensitivity to radiolabeled RNA, which is commonly employed for in-line probing assays. Importantly, μMSA can be used to rapidly measure K_d values as low as 1 nM using fluorescence detection and does not require modification of the riboswitch aptamer structure or the ligand, unlike 2AP fluorescence or FRET experiments.[10−12]

We next determined K_d for the SAM-I *Bs* riboswitch using μMSA and compared our results against those from a conventional in-line probing assay. To determine K_d, RNA peak mobility was measured at different SAM ligand concentrations and the resulting dose response curve was fit with a three-parameter logistic model (Figure 3). μMSA-determined K_d values were 25.226 ± 0.004 nM in tris-borate (TB) buffer with 1 mM Mg^{2+} (TBM1 buffer) (n = 4) and 3.14123 ± 0.00005 nM in TB buffer with 10 mM Mg^{2+} (TBM10 buffer) (n = 4). Both μMSA values agree well with results from the in-line probing assays performed using identical buffer conditions: 25 and 3 nM K_d, respectively (Figures 3 and S4). The observed improvement in ligand binding affinity at 10 mM Mg^{2+} is consistent with biophysical studies that have shown Mg^{2+} facilitates folding of the SAM-I and other riboswitches.[17,30,31]

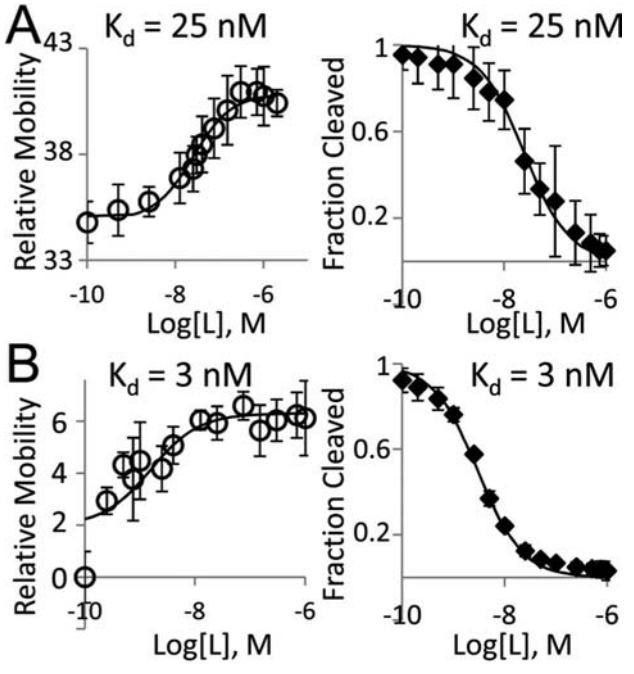

Figure 3. Microfluidic assay can measure K_d for riboswitches with rapid interconversion rates. Riboswitch mobility can be used to extract K_d values that are equivalent to those measured by traditional in-line probing assays. μMSA (left) and slab gel (right) results for the SAM-I *Bs* riboswitch aptamer with (A) TB buffer + 1 mM Mg^{2+} and (B) TB buffer + 10 mM Mg^{2+}. On-chip RNA mobility values (relative to internal standard) are given as $\times 10^{-5}$ $cm^2/(V\ s)$. 0 nM SAM sample was used to determine K_d but plotted at 0.1 nM for on-chip data to allow for logarithmic axis. Solid traces are best-fit three-parameter logistic curves at the K_d shown. Error bars for on-chip data are standard deviation of quadruplicate runs. Error bars for in-line probing assays shown are the standard deviation of values for the sites of modulation analyzed from a single slab gel.

To further probe the effect of Mg^{2+} and K^+ concentration on the RNA mobility shift, we screened varying buffer compositions using μMSA. SAM-I *Bs* riboswitch mobility and the percentage mobility change with saturating amounts of SAM ligand present were measured (Figure 4). A statistically

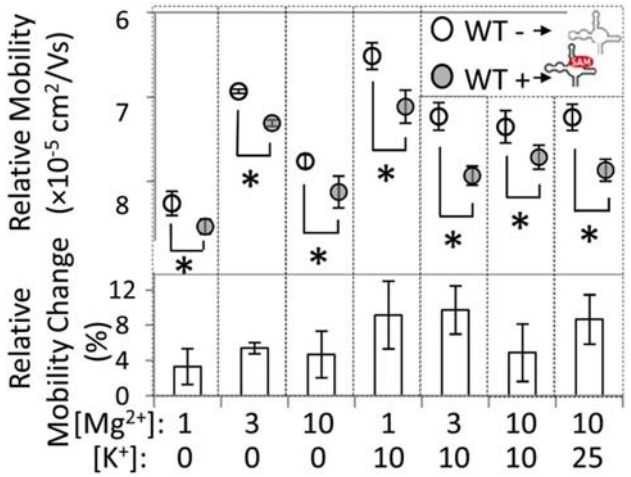

Figure 4. Screening for the effect of Mg^{2+} and K^+ concentration on *Bs* SAM-I riboswitch mobility and the extent of the mobility shift in the presence of SAM ligand. All on-chip mobility shifts are statistically significant using a two tailed t test (p < 0.05) and indicated by '*'. Relative mobility change is the % increase in RNA mobility in the presence of SAM. WT− and WT+ indicate the absence and presence of SAM ligand, respectively. Error bars are standard deviation of triplicate runs. All runs were done in 1× TB buffer with salt concentrations as indicated in mM.

significant ligand-induced shift was observed for all buffer conditions (p < 0.05 using two tailed t test). The relative mobility of the riboswitch did not change according to a consistent trend with increasing Mg^{2+}, either in the presence or absence of monovalent ions. Most likely this is due to the fact that changing ion concentrations affect the interaction of the RNA with electrolyte (run buffer) in the gel matrix[25] as well as potentially the RNA fold. However, the extent of mobility shift upon ligand binding (as measured by relative mobility change) did not appear to be significantly different across the Mg^{2+} concentrations tested. This result is consistent with findings that the SAM-I *Bs* riboswitch assumes an unfolded state in the absence of magnesium, but the magnesium-induced fold is saturated by 1 mM Mg^{2+}.[32] Interestingly, the presence of K+ generally increased the relative mobility change. Unlike the lysine riboswitch, which specifically requires a K^+ ion to chelate the carboxylate group of the amino acid ligand,[33] the SAM-I riboswitch is not known to bind any specific K^+ ions. Thus, the observed effect instead may be attributed to changing the composition of divalent and monovalent ions interacting with the RNA.

As is important for screening, the total time to results using μMSA was notably shorter than the 17 h required for slab gel analysis (Figure S1). Analysis by μMSA required 3.2 min including sample loading and triplicate runs for both samples in order to assess the statistical significance of observed shifts.

dx.doi.org/10.1021/ja310742m | J. Am. Chem. Soc. 2013, 135, 3136−3143

Thus, the time savings achieved with μMSA translates to a 316-fold reduction, critical for high-throughput experimental validation of computationally predicted riboswitch−ligand interactions. As are common yet important advantages of microfluidic design, μMSA requires reduced reagent (amol compared to pmol) and buffer volumes (μL compared to L). Further, μMSA is performed at room temperature, whereas cooling to ≤10 °C is often required to limit diffusion and prevent RNA degradation in long-duration slab gel PAGE.[25] In a practical but important point, the μMSA screening platform allows repeat use of a single PAGE channel for multiple assays that, with proper intermediate wash steps and controls, limit platform preparation time and effort while enabling excellent run-to-run reproducibility. Assay repeatability was evaluated by performing 53 sequential injections of phosphorylase B (PB) over a 2−3 h period. The average time for the peak to migrate 1 mm from the injection junction was 9.6 ± 0.2 s, representing a 2.3% variation. The average peak height over 46 sequential injections was 1.80 ± 0.28 fluorescence units, representing a 15% variation. μMSA gels were used for an average of 62 runs over a 7 month period of experimentation. This high repeatability is expected owing to the low nonspecific adsorption and durability of the PA gels.

Quantitative Analysis of Slowly Interconverting Riboswitch States: A Putative SAM-I Riboswitch from *Polaribacter irgensii*. We next studied the mobility shift and assessed the K_d for a riboswitch that slowly interconverts between bound and free states. Here a putative SAM-I riboswitch isolated from *Polaribacter irgensii* (*Pi*) was analyzed via μMSA for ligand binding with increasing concentrations of SAM ligand. Both the μMSA and slab gel mobility shift assays reported two *Pi* riboswitch peaks for ligand:riboswitch ratios of <1 (Figure 5A,B). In these cases, the riboswitch is present in excess over ligand, and the bound and unbound populations are resolved as separate peaks (measured on-chip R_s = 0.66), demonstrating that negligible interconversion is occurring during the time scales of both the μMSA and slab gel separations. The μMSA required a 12 s separation step, while the slab gel format required appreciably longer (a 20 h separation step). The short μMSA analysis times mitigate diffusive band broadening found in long-duration slab gel native PAGE.[25] μMSA reports sharp peaks even under native PAGE conditions. Quantifying the amount of material in each conformational state should thus benefit from native PAGE in microfluidic formats.

In this system, the ligand-bound riboswitch population increases with ligand concentration until all RNA molecules are in the bound state, as predicted (Figure 1). We used the μMSA to generate a dose−response curve then fit that experimental data with a three-parameter logistic model to yield K_d (Figure 5C). The notable difference between our analysis here and that of the fast interconversion regime is that we now measure the peak height for the higher mobility peak (ligand-bound population) across increasing ligand concentrations and not the mobility shift of a single peak as in the rapid interconversion regime. With this approach, the K_d of SAM-I *Pi* was measured as 1.0 ± 0.2 nM using μMSA (n = 4), which is on the order of the 3 nM value measured using a conventional in-line probing assay (Figures 5D and S5). Deviation between the two methods may arise from optimization demands on the peak fitting algorithm and/or fluorescently labeled RNA concentration inaccuracies.

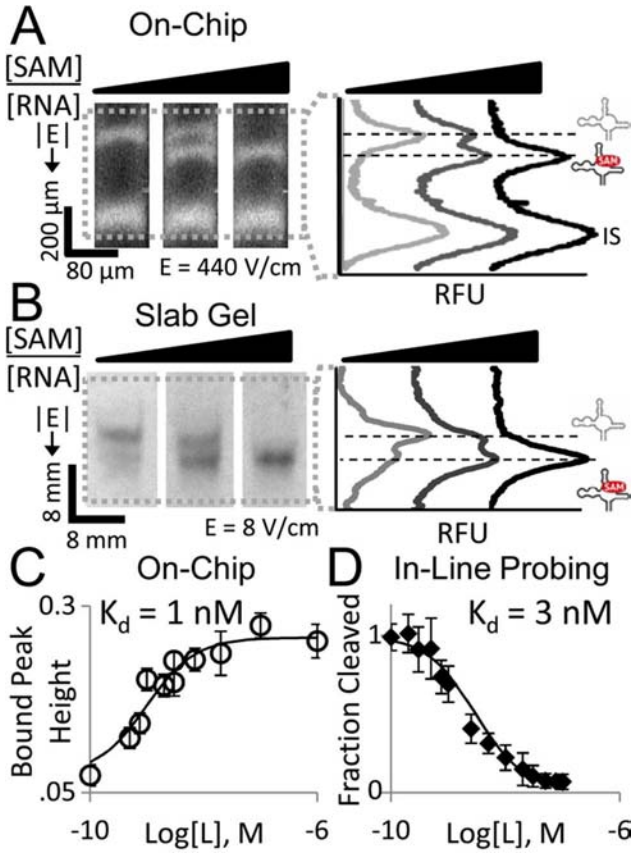

Figure 5. Microfluidic assay can measure K_d for slowly interconverting riboswitches. Two peaks are resolved on (A) μMSA and (B) slab gel formats representing bound and unbound SAM-I *Pi* riboswitch populations with the amount of the bound form of the riboswitch increasing as SAM concentration increases. PB internal standard (IS) peak is at 1.6 mm separation distance on-chip. (C) Bound riboswitch peak height can be used to extract K_d values that are equivalent to those measured by traditional in-line probing assays (D). On-chip error bars represent the standard deviation of quadruplicate runs. Error bars for in-line probing assay are the standard deviation of values for the sites of modulation analyzed from a single slab gel. 0 nM SAM sample was used to determine K_d but plotted at 0.1 nM in (C) to allow for logarithmic axis. 1× TB + 10 mM Mg^{2+} in gel and run buffers.

As is critical to an efficient mobility shift screening platform, measurement of riboswitch−ligand K_d for one riboswitch−ligand pair required 1.87 h for μMSA versus 44+ hours using the in-line probing assay. Use of μMSA resulted in (at a minimum) a 24-fold reduction in the time-to-results. The total time to results for the microfluidic format includes a 1 h sample incubation to equilibrate the binding reaction and 52 min to run 12 samples on-chip in quadruplicate. Meanwhile the in-line probing method requires a 40 h sample incubation to perform the in-line cleavage reaction after ligand binding has equilibrated, followed by a 2−4 h denaturing PAGE slab gel run, an additional 2 h to dry the gel and several hours to overnight to image the gel using a phosphorimager cassette.

Microfluidic Screening for Candidate Riboswitch Validation. Efficient screening of computationally predicted riboswitches for functionality is critical for increasing the number of known riboswitch−ligand pairs. To this end, we assayed five computationally predicted but previously unvalidated SAM-I riboswitches using μMSA in the presence and absence of SAM ligand (Figure 6). The computationally

dx.doi.org/10.1021/ja310742m | J. Am. Chem. Soc. 2013, 135, 3136−3143

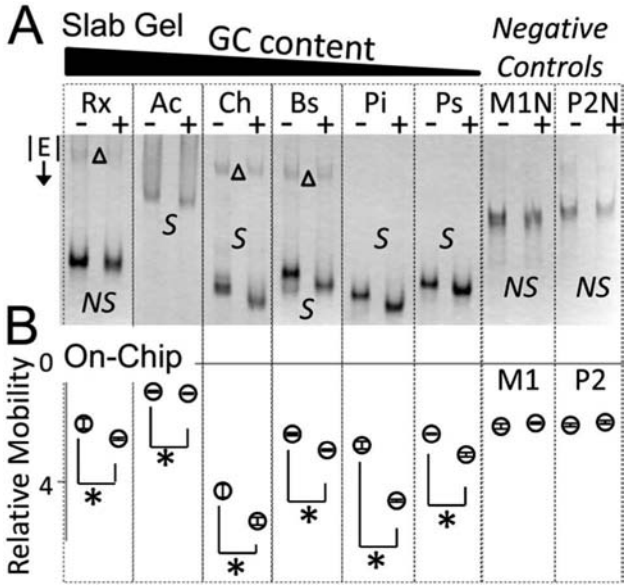

Figure 6. Microfluidic precision enables mobility shift as metric for screening candidate riboswitch function. The improved resolution of the microfluidic mobility shift assay over conventional slab gel mobility shift assays allows detection of GC-rich putative SAM-I riboswitches. (A) 'S' indicates a shift and 'NS' indicates no shift. (B) All on-chip mobility shifts are statistically significant using a two tailed t test ($p < 0.05$) and indicated by '*'. Error bars represent standard deviation of triplicate runs. M1, M1N, P2, and P2N mutants do not demonstrate a shift, as expected. See Figure S1 for slab gel data on M1 and P2 mutants. Upper bands in slab gel ('Δ') appear to be nonbinding RNA conformers. Slab gel E = 8 V/cm, on-chip E = 240 V/cm. 1× TB + 10 mM Mg^{2+} in gel and run buffers. Relative mobility values are $\times 10^{-3}$ $cm^2/(V\ s)$.

predicted putative SAM-I riboswitches were selected for their varying properties (e.g., GC content, length) and were isolated from *Rubrobacter xylanophilus* (*Rx*), *Acidothermus cellulolyticus* (*Ac*), *Carboxydothermus hydrogenoformans* (*Ch*), *Pi* (discussed above), and *Polaribacter sp.* (*Ps*). Selection criteria are provided in SI.

A statistically significant mobility shift was measured for all five putative SAM-I riboswitches from *Rx*, *Ac*, *Ch*, *Pi*, and *Ps* using μMSA ($p < 0.05$ using two tailed t test, indicated with a '*' in Figure 6B). The slab gel format detected a mobility shift for four of the five putative SAM-I riboswitches. No mobility shift was observed for the GC-rich SAM-I riboswitch from *Rx* (indicated with 'NS' in Figure 6A). The statistical significance of an observed shift could not be calculated with the slab gel format owing to the high variability and long assay run times. The well-studied SAM-I riboswitch from *Bs* was included as a positive control and demonstrated a mobility shift on both formats, as expected. M1 and P2 are previously characterized mutants of the *Bs* SAM-I riboswitch[18,28] (also characterized in Figure S1) that do not bind SAM ligand and were included as negative controls for on-chip experiments. The related M1N and P2N mutants, which contain some additional flanking sequences, were used as separate negative controls for slab gel experiments. Each demonstrated no statistically significant mobility shift in equally powered experiments. These results suggest that μMSA enables detection of a mobility shift for smaller conformational changes, including challenging riboswitch aptamer structures with high GC content (up to 75% GC demonstrated here with *Rx*) and long chain lengths which result in a smaller shift relative to the total size of the molecule (up to 162 nt considered here with *Ac*). Mobility shift detection can be improved on a slab gel format by increasing well size, but importantly, sample throughput is sacrificed (Figure S6).

The total time to screen the five candidate riboswitches, one positive control, and two negative controls via μMSA was 58 min. The time savings and repeatability attained with μMSA enabled replicates thus allowing determination of statistical significance for an observed shift, an endeavor that is not typically performed with conventional slab gels.

■ CONCLUSIONS

Taken together, the μMSA microfluidic screening tool introduced here opens the possibility of facile library screens for selection and validation of novel riboswitches. The demonstrated rapid assay times and precise quantitative capabilities enable the mobility resolution required to measure K_d for both slowly and rapidly interconverting riboswitch–ligand pairs. Owing to the analytical improvements of μMSA over slab gel formats and the prevalent usage of slab gel mobility shift assays in riboswitch research, ongoing work in our laboratories focuses on utilizing μMSA to study other riboswitches beyond SAM-I. The μMSA format has wide-ranging analytical potential, such as: facilitating the identification of natural metabolite targets for orphan riboswitch classes for which no ligand has been discovered to date;[34] enabling the screening of conditions (e.g., buffer composition, ligand libraries) for riboswitch–ligand binding and selection experiments; allowing efficient characterization of the binding affinity and kinetics of newly discovered riboswitch–ligand pairs; and providing insight into the concentrations of ligand needed in the cell to induce genetic regulation for thermodynamically controlled riboswitches. Microfluidic assay design may also advance the identification of new riboswitch–ligand pairs with broad applications in antibiotic development[4] and new genetic regulation control[5] and for use as biosensors for metabolite sensing *in vivo*.[6]

■ EXPERIMENTAL PROCEDURES

Reagents and Oligonucleotides. RNAs were transcribed *in vitro* using standard protocols[35] from DNA templates containing the extended T7 promoter sequence generated by PCR. Fluorophore dyes (fluorescein, AlexaFluor 488, or AlexaFluor 633) were conjugated to the RNAs following standard procedures for 3′ end labeling.[36] Additional details on preparation of DNA constructs and 3′ end labeled fluorescent RNAs are given in SI.

Binding reaction samples for μMSA were prepared by adding RNA, SAM ligand (as indicated), 2× TB buffer, and dI water in a LoBind eppendorf tube at the indicated concentrations, heating at 70 °C for 3 min, cooling for 10 min to avoid denaturing the internal standard(s), adding internal standard(s), and equilibrating at room temperature for 1 h in the dark. Additional details on protein and chemical reagents are included in SI.

Microfluidic Device Fabrication. Optical white soda lime glass microfluidic chips were fabricated with standard wet etch processing by Caliper Life Sciences (Hopkinton, MA). Photopatterning of polymer structures and sieving matrixes in the glass channels were conducted in-house. Open channels were washed and silanized using 3-(trimethoxysilyl)-propyl methacrylate (98%) (Sigma Aldrich, St. Louis, MO) as described previously.[27] Additional details are included in SI. 3–10%T and 3–12%T discontinuous PA gel architectures were utilized in this work to match the conditions typically used in slab gel formats. The stacking interface has also been shown to increase resolving power.[15]

dx.doi.org/10.1021/ja310742m | J. Am. Chem. Soc. 2013, 135, 3136–3143

μMSA Operation. The μMSA utilizes PA gel photopatterned in 80 × 20 μm microfluidic channels that intersect in a 't' pattern.[37−39] PA gel-containing glass chips were secured in a custom-built Delrin manifold to expand the reservoirs for each well and minimize external light. The riboswitch and ligand pair were incubated off-chip and 2 μL of sample was pipetted into the sample well (S, Figure 1). All other wells were filled with 50 μL of 1× TB buffer with the appropriate Mg^{2+} and K^+ concentration. Voltage and current monitoring and control at each well were accomplished using a custom built, eight channel high-voltage power supply with current/voltage feedback control. Platinum electrodes were inserted into each well. Electrophoretic sample loading was accomplished by applying −3 μA to S, 0 μA to buffer (B), and buffer waste (BW), and grounding well sample waste (SW) for ∼1 min (E ∼ 130 V/cm loading). Electrophoretic separation was initiated by switching the electric field orthogonally to apply −5 μA to well B, 0 μA to S and SW, and grounding well BW (E ∼ 240−530 V/cm in separation channel). In this step, a plug of sample was injected into the separation channel (B−BW), and the riboswitch and internal standards were allowed to migrate and resolve according to their electrophoretic mobilities.

Imaging and Data Analysis. Full-field images of migration and concentration distributions of separating fluorescent analytes were measured via an IX-70 inverted epi-fluorescent microscope and charge-coupled device (CCD) camera setup. All microfluidic K_d constants were measured using an inverted laser-induced fluorescence (LIF) microscope. Additional details on the LIF system, microscope setup, and image processing, are given in SI.

The separation resolution (R_s) metric reports the ability to resolve riboswitch populations using PAGE. When R_s < 0.5 and two peaks were expected owing to the presence of ligand, peaks were deemed unresolved, and rapid interconversion was assumed. Rapidly interconverting riboswitch K_d was calculated by fitting a three-parameter logistic fit binding equation of the form $y = \beta_1 \times [SAM]/(K_d + [SAM]) + \beta_3$ to a relative mobility (μ_{rel}) dose response curve, where μ_{rel} is RNA mobility relative to an internal standard. More information on the calculation of μ_{rel} and fitted parameters are given in SI.

When R_s > 0.5, peaks were deemed resolved, and slow interconversion was assumed. Riboswitch K_d was calculated by fitting a three-parameter logistic fit binding equation to the bound peak height dose response curve. Peak height measurements were extracted with a nonlinear Gaussian peak fitting algorithm (GaussAmp) using OriginPro 8.5 (OriginLab, Northampton, MA). More information on the calculation of peak height and fitted variables are given in SI.

Design and Modeling of Assay Parameters. To rationally choose the assay parameters and understand the performance improvements gained by moving to a microfluidic format, we compared the Da_{on} and Da_{off} values that are accessible to slab gels and microfluidic formats for given association and dissociation rates. Bound and unbound riboswitch separation resolution was computationally extracted for varying k_{on} and k_{off} values. Simulations were written and performed in Matlab (Mathworks, Natick, MA). Additional details on the model are included in SI and Figure S2.

Analysis of RNA−Ligand Interactions by Slab Gel Native PAGE. While protected from light, 1−3 pmol fluorescently labeled RNA in 20 μL of TBM10 buffer (90 mM Tris, 89 mM boric acid, 10 mM $MgCl_2$, pH 8.5) was renatured by heating to 70 °C on a heat block for 3 min followed by a quick table-top centrifugation and slow cooling to room temperature for 1 h. Renaturation of the RNA was performed in either the presence (500 nM or 5 μM) or absence of SAM. The 10%T gel was run with recirculating TBM10 buffer at 4 °C at 200 V (electric field of 8 V/cm) for 17−20 h in the dark. Additional details on run and imaging conditions are given in SI. AlexaFluor 488-labeled bovine serum albumin (BSA) or trypsin inhibitor (TI) were used as internal standards and exhibited slower and faster mobility, respectively, than the RNA or RNA−ligand complex.

Analysis of RNA−Ligand Interactions by In-Line Probing Assay. Ligand binding analysis was performed following standard in-line probing procedures[9] with modifications to the buffer conditions to match the conditions used for native PAGE. Additional details are given in SI.

To determine K_d, sites were identified whose pattern of spontaneous cleavage changed upon ligand binding. For each of these sites of modulation, the signal intensity was normalized to the observed value at the highest ligand concentration. The fraction of RNA cleaved at each ligand concentration, which corresponds to the fraction of unbound RNA, was taken as the average of the data analyzed for several sites of modulation. The dissociation constant was determined by fitting the experimental data to a best-fit curve for a 1:1 RNA−ligand complex. In-line probing assays for *Bs* and *Pi* SAM-I riboswitches and the mapped secondary structure of *Pi* SAM-I riboswitch are given in Figures S4 and S5.

Analysis of RNA−Ligand Interactions by μMSA. *Screening of Mg^{2+} and K^+ Concentrations.* All buffer screening experiments were done with 3−12%T microfluidic gel architectures fabricated in the appropriate buffer. Full-field imaging was done on the IX-70 inverted epi-fluorescence microscope setup. 1× TB buffer with 1 mM Mg^{2+}, 3 mM M^{2+}, 10 mM Mg^{2+}, 1 mM Mg^{2+} and 10 mM K^+, 3 mM Mg^{2+} and 10 mM K^+, 10 mM Mg^{2+} and 10 mM K^+, and 10 mM Mg^{2+} and 25 mM K^+ concentrations were screened. All microfluidic assays in this study utilized a 3−12%T gel architecture fabricated in the appropriate buffer. Statistical significance of a mobility shift was assessed using a two tailed t test (p < 0.05, n = 3). Additional details are given in SI.

Screening of Candidate Riboswitch Functionality. Ligand binding and the resultant conformational change of candidate SAM-I riboswitches *Rx*, *Ac*, *Ch*, *Bs*, *Pi*, and *Ps* were assessed on-chip as described above using full-field imaging on the inverted epi-fluorescence IX-70 microscope. Fluorescein-labeled SAM-I mutant riboswitches M1 and P2 (on-chip) and M1N and P2N (slab gel) were run as negative controls. Additional details are in SI. Riboswitch mobility shifts were assessed by comparing riboswitch mobility in no ligand and saturating ligand (7.1 μM) conditions. Statistical significance of the mobility shift was assessed using a two tailed t test (p < 0.05, n = 3). A 3−10%T gel architecture was used, and TBM10 buffer was used in the sample, gel, and run buffers.

■ ASSOCIATED CONTENT

Supporting Information

Quantitative benefit of μMSA, binding and electrokinetic transport model, critical R_s calculation, in-line probing assay results, slab gel mobility resolution, details on methods and experimental setup, sequences of DNA constructs and primers. This material is available free of charge via the Internet at http://pubs.acs.org.

■ AUTHOR INFORMATION

Corresponding Author

mingch@berkeley.edu; aeh@berkeley.edu

Notes

The authors declare no competing financial interest.

■ ACKNOWLEDGMENTS

This work is supported by NIH New Innovator Awards (grant no. 1DP2OD007294 to A.E.H. and grant no. 1DP2OD008677 to M.C.H.), a NIH NRSA Training Grant in Chemical Biology (J.V., S.F.H.), and a NSF CBET CAREER Award (grant no. 1056035 to A.E.H.). The authors would also like to acknowledge Jonathan L. McMurry for technical assistance and Augusto M. Tentori for helpful discussion. K.K. is a National Science Foundation Graduate Research Fellow. M.C.H. holds a Career Award at the Scientific Interface from the Burroughs Wellcome Fund. A.E.H. is a Sloan Foundation Research Fellow in chemistry.

REFERENCES

(1) Breaker, R. R. *Mol. Cell* **2011**, *43*, 867.
(2) Henkin, T. M. *Genes Dev.* **2008**, *22*, 3383.
(3) Nahvi, A.; Sudarsan, N.; Ebert, M. S.; Zou, X.; Brown, K. L.; Breaker, R. R. *Chem. Biol.* **2002**, *9*, 1043.
(4) Blount, K. F.; Breaker, R. R. *Nat. Biotechnol.* **2006**, *24*, 1558.
(5) Dixon, N.; Duncan, J. N.; Geerlings, T.; Dunstan, M. S.; McCarthy, J. E. G.; Leys, D.; Micklefield, J. *Proc. Natl. Acad. Sci. U.S.A.* **2010**, *107*, 2830.
(6) Paige, J. S.; Nguyen-Duc, T.; Song, W.; Jaffrey, S. R. *Science* **2012**, *335*, 1194.
(7) Weinberg, Z.; Barrick, J. E.; Yao, Z.; Roth, A.; Kim, J. N.; Gore, J.; Wang, J. X.; Lee, E. R.; Block, K. F.; Sudarsan, N. *Nucleic Acids Res.* **2007**, *35*, 4809.
(8) Weinberg, Z.; Wang, J. X.; Bogue, J.; Yang, J.; Corbino, K.; Moy, R. H.; Breaker, R. R. *Genome Biol.* **2010**, *11*, R31.
(9) Regulski, E. E.; Breaker, R. R. *Methods Mol. Biol.* **2008**, *419*, 53.
(10) Shanahan, C. A.; Gaffney, B. L.; Jones, R. A.; Strobel, S. A. *J. Am. Chem. Soc.* **2011**, *133*, 15578.
(11) Heppell, B.; Mulhbacher, J.; Penedo, J. C.; Lafontaine, D. A. *Methods Mol. Biol.* **2009**, *540*, 25.
(12) Haller, A.; Rieder, U.; Aigner, M.; Blanchard, S. C.; Micura, R. *Nat. Chem. Biol.* **2011**, *7*, 393.
(13) Gilbert, S. D.; Batey, R. T. *Methods Mol. Biol.* **2009**, *540*, 97.
(14) Roth, A.; Winkler, W. C.; Regulski, E. E.; Lee, B. W. K.; Lim, J.; Jona, I.; Barrick, J. E.; Ritwik, A.; Kim, J. N.; Welz, R. *Nat. Struct. Mol. Biol.* **2007**, *14*, 308.
(15) Hou, C.; Herr, A. E. *Anal. Chem.* **2010**, *82*, 3343.
(16) Fried, M. G. *Electrophoresis* **1989**, *10*, 366.
(17) Chen, B.; Zuo, X.; Wang, Y. X.; Dayie, T. K. *Nucleic Acids Res.* **2012**, *40*, 3117.
(18) Heppell, B.; Lafontaine, D. A. *Biochemistry* **2008**, *47*, 1490.
(19) Miller, O. J.; El Harrak, A.; Mangeat, T.; Baret, J. C.; Frenz, L.; El Debs, B.; Mayot, E.; Samuels, M. L.; Rooney, E. K.; Dieu, P. *Proc. Natl. Acad. Sci. U.S.A.* **2012**, *109*, 378.
(20) Chung, K.; Kim, Y.; Kanodia, J. S.; Gong, E.; Shvartsman, S. Y.; Lu, H. *Nat. Methods* **2010**, *8*, 171.
(21) Lecault, V.; VanInsberghe, M.; Sekulovic, S.; Knapp, D. J. H. F.; Wohrer, S.; Bowden, W.; Viel, F.; McLaughlin, T.; Jarandehei, A.; Miller, M. *Nat. Methods* **2011**, *8*, 581.
(22) Nagrath, S.; Sequist, L. V.; Maheswaran, S.; Bell, D. W.; Irimia, D.; Ulkus, L.; Smith, M. R.; Kwak, E. L.; Digumarthy, S.; Muzikansky, A. *Nature* **2007**, *450*, 1235.
(23) Goodrich, J. A.; Kugel, J. F. *Binding and Kinetics for Molecular Biologists*; Cold Spring Harbor Laboratory Press: Cold Spring Harbor, NY, 2007.
(24) Giddings, J. C. *Unified Separation Science*; Wiley: New York: New York, 1991.
(25) Woodson, S. A.; Koculi, E. *Methods Enzymol.* **2009**, *469*, 189.
(26) Cann, J. R. *Anal. Biochem.* **1996**, *237*, 1.
(27) Karns, K.; Herr, A. E. *Anal. Chem.* **2011**, *83*, 8115.
(28) Winkler, W. C.; Nahvi, A.; Sudarsan, N.; Barrick, J. E.; Breaker, R. R. *Nat. Struct. Biol.* **2003**, *10*, 701.
(29) Ying, B. W.; Fourmy, D.; Yoshizawa, S. *RNA* **2007**, *13*, 2042.
(30) Hayes, R. L.; Noel, J. K.; Mohanty, U.; Whitford, P. C.; Hennelly, S. P.; Onuchic, J. N.; Sanbonmatsu, K. Y. *J. Am. Chem. Soc.* **2012**, *134*, 12043.
(31) Batey, R. T.; Gilbert, S. D.; Montange, R. K. *Nature* **2004**, *432*, 411.
(32) Heppell, B.; Blouin, S.; Dussault, A. M.; Mulhbacher, J.; Ennifar, E.; Penedo, J. C.; Lafontaine, D. A. *Nat. Chem. Biol.* **2011**, *7*, 384.
(33) Serganov, A.; Huang, L.; Patel, D. J. *Nature* **2008**, *455*, 1263.
(34) Meyer, M. M.; Hammond, M. C.; Salinas, Y.; Roth, A.; Sudarsan, N.; Breaker, R. R. *RNA Biol.* **2011**, *8*, 5.
(35) Rio, D. C.; Ares, M.; Nilsen, T. W. *RNA: A laboratory manual*; Cold Spring Harbor Laboratory Press: Cold Spring Harbor, NY, 2010.
(36) Willkomm, D.; Hartmann, R.; Bindereif, A.; Schon, A.; Westhof, E. *Handbook of RNA Biochemistry*; Wiley, 2005; Vol. *1*.
(37) Herr, A. E.; Singh, A. K. *Anal. Chem.* **2004**, *76*, 4727.
(38) Apori, A. A.; Herr, A. E. *Anal. Chem.* **2011**, *83*, 2691.
(39) Colyer, C. L.; Mangru, S. D.; Harrison, D. J. *J. Chromatogr., A* **1997**, *781*, 271.